Microplasma-Assisted Growth of Colloidal Silver Nanoparticles for Enhanced Antibacterial Activity

Ruixue Wang, Shasha Zuo, Weidong Zhu, Shan Wu, Weifeng Nian, Jue Zhang,* Jing Fang

This paper presents a one-step method for the rapid synthesis of colloidal silver nanoparticles (AgNPs) for bacterial disinfection. Silver ions were electrochemically reduced to silver atoms in an $AgNO_3$ solution with the assistance of an atmospheric argon microplasma jet. Dextran was used to stabilize the AgNPs in the liquid solution. Ultraviolet–visible spectroscopy, transmission electron microscopy, atomic force microscopy, and Fourier transform infrared spectroscopy were used to characterize the synthesized AgNPs. It was found that the size of the nanoparticles can be controlled by adjusting the dextran monomer/Ag^+ molar ratio in the solution. Furthermore, antibacterial activity of the as-synthesized AgNPs against *Escherichia coli* and *Staphylococcus aureus* was carried out in liquid as well as on solid growth media, as a function of the AgNPs concentration. The results showed that the AgNPs had a significant antibacterial activity against those bacteria cells and the minimum inhibition concentration was associated with the type of bacteria and initial bacterial concentration.

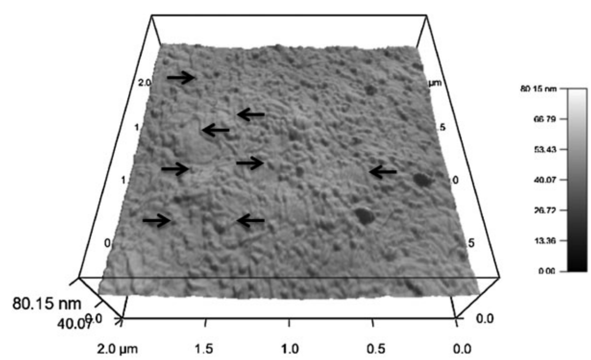

1. Introduction

The antibacterial effects of silver and silver salts have been noticed since ancient time.[1–3] But only until recently, Ag nanoparticles (AgNPs) have attracted much attention due to their superior antibacterial property, which is attributed to their high specific surface area, and high fraction of surface atoms.[4–7] It is found that the antibacterial activities of AgNPs are related to their sizes: smaller AgNPs release more Ag^+ ions and are more antibacterial.[8,9] A variety of methods have been reported to synthesize AgNPs with desirable size, including physical, chemical, and biological methods.[10–12] Among these methods, chemical reduction is the most popular approach for the production of nanoparticles.[13–15] However, most chemical methods cannot avoid the use of toxic chemicals in the synthesis process.[8] Since noble metal nanoparticles such as gold, silver, and platinum nanoparticles are widely applied to human contacting areas, environmentally friendly processes of nanoparticle synthesis are always of high preference.[16]

Plasma–liquid processes at atmospheric pressure have drawn much attention as a novel nanoparticle synthesis

R. Wang, S. Zuo, W. Nian, Prof. J. Zhang, J. Fang
Academy for Advanced Interdisciplinary Studies, Peking University, Beijing 100871, P. R. China
E-mail: zhangjue@pku.edu.cn
W. Zhu
Department of Applied Science and Technology, Saint Peter's University, Jersey City, New Jersey 07306, USA
S. Wu, Prof. J. Zhang, J. Fang
College of Engineering, Peking University, Beijing 100871, P. R. China

Plasma Process. Polym. **2014**, *11*, 44–51

DOI: 10.1002/ppap.201300038

strategy in the past a few years due to their simplicity and environmental friendliness.[17–19] By reducing the critical dimensions of the devices down to micrometer range enables plasma to be sustained at atmospheric pressure and room temperature.[20] The high density of electrons with energies in excess of 10 eV present in these plasmas allows the reduction of metal cations in aqueous phase.[21] Compared to traditional electrochemical method, the nanoparticle synthesis using the plasma–liquid interfaces is especially advantageous since the reducing agent – the atmospheric pressure non-thermal plasma is generated above the grounded electrolyte, which in term avoids the difficulty of nanoparticle production isolation. Additionally, toxic stabilizers and reducing agents are unnecessary in the process and the synthesis of nanoparticles is continuous during the plasma irradiation.[22,23]

A few groups have recently reported the generation of silver nanoparticles in liquid using this method.[24–26] However, the studies for mechanisms and generation of size-controllable silver nanoparticles based on plasma–liquid interaction are still limited. In addition, the antimicrobial property of the as-synthesized AgNPs by this method is rarely studied. In this paper, we report the preparation of colloidal silver nanoparticles with plasma–liquid process for bacterial disinfection. Silver ions were electrochemically reduced by an atmospheric non-thermal argon microplasma. Dextran was added to protect the AgNPs and the particle sizes were controlled by altering dextran monomer/Ag^+ molar ratios. The structure, morphology, and properties of the resulting AgNPs were characterized by Ultraviolet–visible (UV–Vis) spectroscopy, transmission electron microscopy (TEM), atomic force microscopy (AFM), and Fourier transform infrared (FTIR) spectroscopy. Antibacterial activity of the synthesized AgNPs against *Escherichia coli* and *Staphylococcus aureus* was also investigated.

2. Experimental Section

2.1. Synthesis of Silver Nanoparticles

The experimental set-up for the microplasma-assisted synthesis of AgNPs is modeled after reference [24]. As shown in the schematic diagram in Figure 1, the reaction was performed in a U-shaped electrochemical cell, which consisted of a platinum (Pt) anode and a microplasma cathode. All chemicals were of analytical grade and were used without further purification. The electrolytic solutions consisted of $AgNO_3$ (5 mM) and dextran (Mw 4 000 Da). The solution was separated into anolyte and catholoyte by a cation exchange membrane at the bottom of the cell. A copper capillary tube (~7 cm long with pore size of 0.355 mm in diameter, KS Engineering, US) was positioned at ~1 mm above the surface of the solution and was pressurized with argon (Ar 99.99 purity) gas at a constant flow rate of 50 SCCM (standard cubic centimeter per minute). The electrochemical cell was driven by a direct current negative-polarity high-voltage power supply (Matsuada AU5R120) through a 5.1 kΩ ballast resistor. Upon the application of the DC high voltage, a microplasma filament formed in the space between the end of the copper capillary tube and the surface of the solution. The microplasma discharge was sustained at a voltage around 400 V with an operating current of 13 mA. During the reaction, the pH values of the anolyte and catholyte were evaluated with a Microprocessor pH-meter (HANNA, pH123 Instruments, USA).

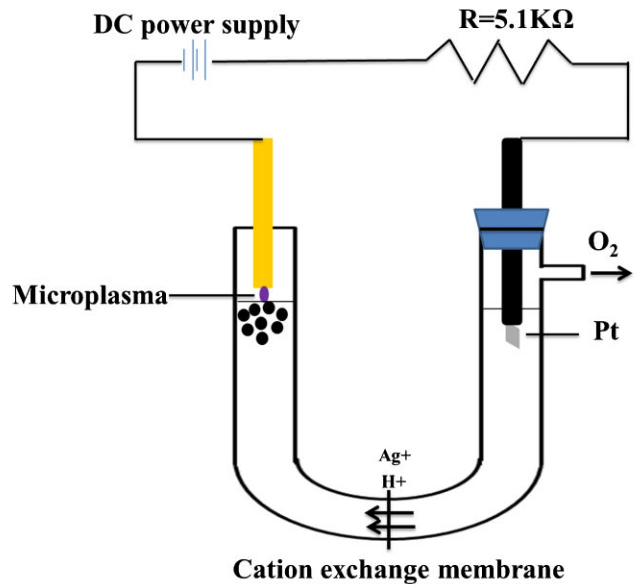

Figure 1. A schematic diagram of the electrochemical cell with an atmospheric-pressure non-thermal microplasma cathode and a Pt foil anode.

2.2. Characterization

The resultant AgNPs (in the reaction medium) were characterized by an ultraviolet–visible absorption spectrometer (UV–Vis, UV-2450, SHIMADZU, Japan) in the wavelength range from 200 to 800 nm. Their size and morphology were evaluated via an AFM (Asylum Research, USA) and a transmission electron microscope (TEM, TECNAI F20, USA). FTIR absorption spectroscopy was performed over 400–4 000 cm^{-1} on a Nexus mode-670 spectrometer in the diffuse reflectance mode at a resolution of 2 cm^{-1}.

2.3. Antibacterial Test

The AgNPs' bactericidal effect depends on the concentration of the nanoparticles in the liquid and the initial bacterial concentration.[27] *E coli* and *S. aureus* of initial concentrations of 10^6 and 10^8 CFU ml^{-1} were exposed to twofold serial dilutions of the AgNPs (from 0 to 100 $\mu g\ ml^{-1}$) in Luria–Bertani (LB) medium. The cultures were incubated at 37 °C and shaken at 180 rpm. Growth rates and bacterial concentrations were determined by measuring the optical density (OD) at 600 nm using a UV–Vis spectrophotometer (Unico7200, China) every 2 h up to 16 h. Samples treated with AgNPs after 16 h were spread on nutrient agar plates. After

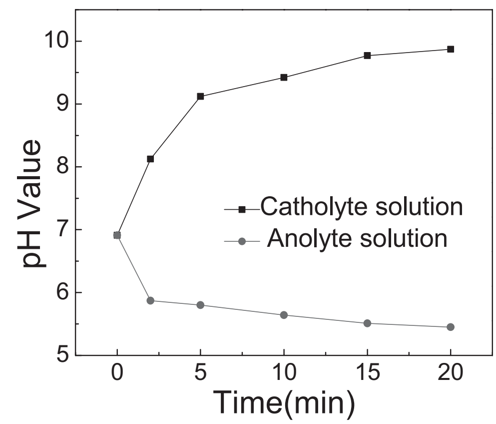

Figure 2. pH values of cathode and anode solution for different plasma treatment time.

incubation at 37°Cfor 24 h, the minimum inhibition concentration (MIC) was determined by counting colony formation units (CFUs) on the agar plates.

3. Results

3.1. Synthesis of Silver Nanoparticles

Once the microplasma was ignited, the solution immediately under the microplasma quickly became yellow, indicating the effective formation of AgNPs. The process of the nanoparticle synthesis involves five steps, which were described below:

1. Release of the oxygen gas on the anode:

$$2H_2O - 4e^- \rightarrow O_2 \uparrow + 4H^+ \quad (1)$$

2. Reductive formation of zero-valent Ag atoms in liquid below the microplasma cathode:

$$Ag^{+1} + e^- \rightarrow Ag^0 \quad (2)$$

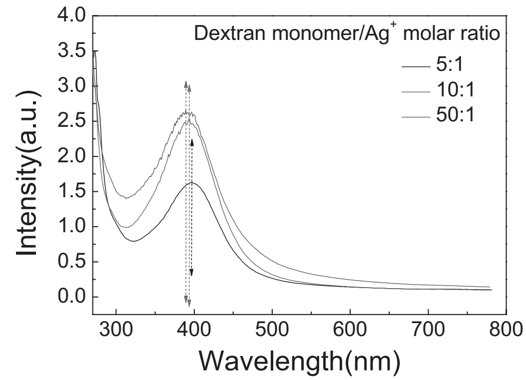

Figure 4. UV–Vis absorption spectra of the AgNPs containing electrolytic solutions after a reaction time of 5 min with dextran monomer/Ag^+ molar ratio of 5:1, 10:1, and 50:1, respectively.

And release of the hydrogen gas:

$$2H_2O + 2e^- \rightarrow H_2 \uparrow + 2OH^- \quad (3)$$

3. Ag^+ and H^+ ions migration to the cathode;
4. Formation of silver nanoparticles via nucleation and growth due to attractive van der Waals forces between Ag atoms;
5. The synthesized silver nanoparticles were coordinated with hydroxyl group of dextran molecule preventing their large-scale aggregation.[28]

The above-described reactions were further confirmed by monitoring the pH value of catholyte and anolyte with a microprocessor pH meter at different reaction times. The results are shown in Figure 2. In this condition, dextran monomer/Ag^+ molar ratio of 5:1 were used. After 20 min, the pH value of catholyte solution increased to approximately 9.87 and anolyte solution decreased to 5.45, due to the generation of $OH^-$and H^+ [formula (1) and (3)], respectively.

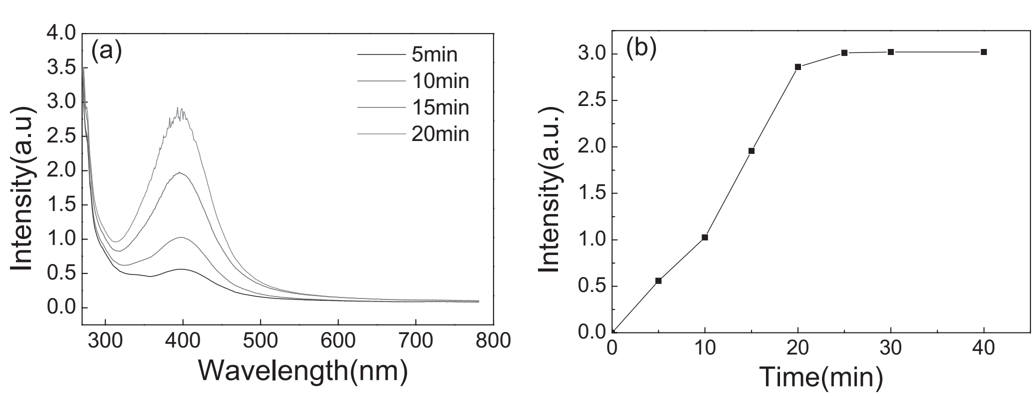

Figure 3. (a) UV–Vis absorption spectra of AgNP containing electrolytic solution after a reaction time of 5, 10, 15, and 20 min, respectively; (b) time dependence of the absorption intensity at 396 nm.

DOI: 10.1002/ppap.201300038

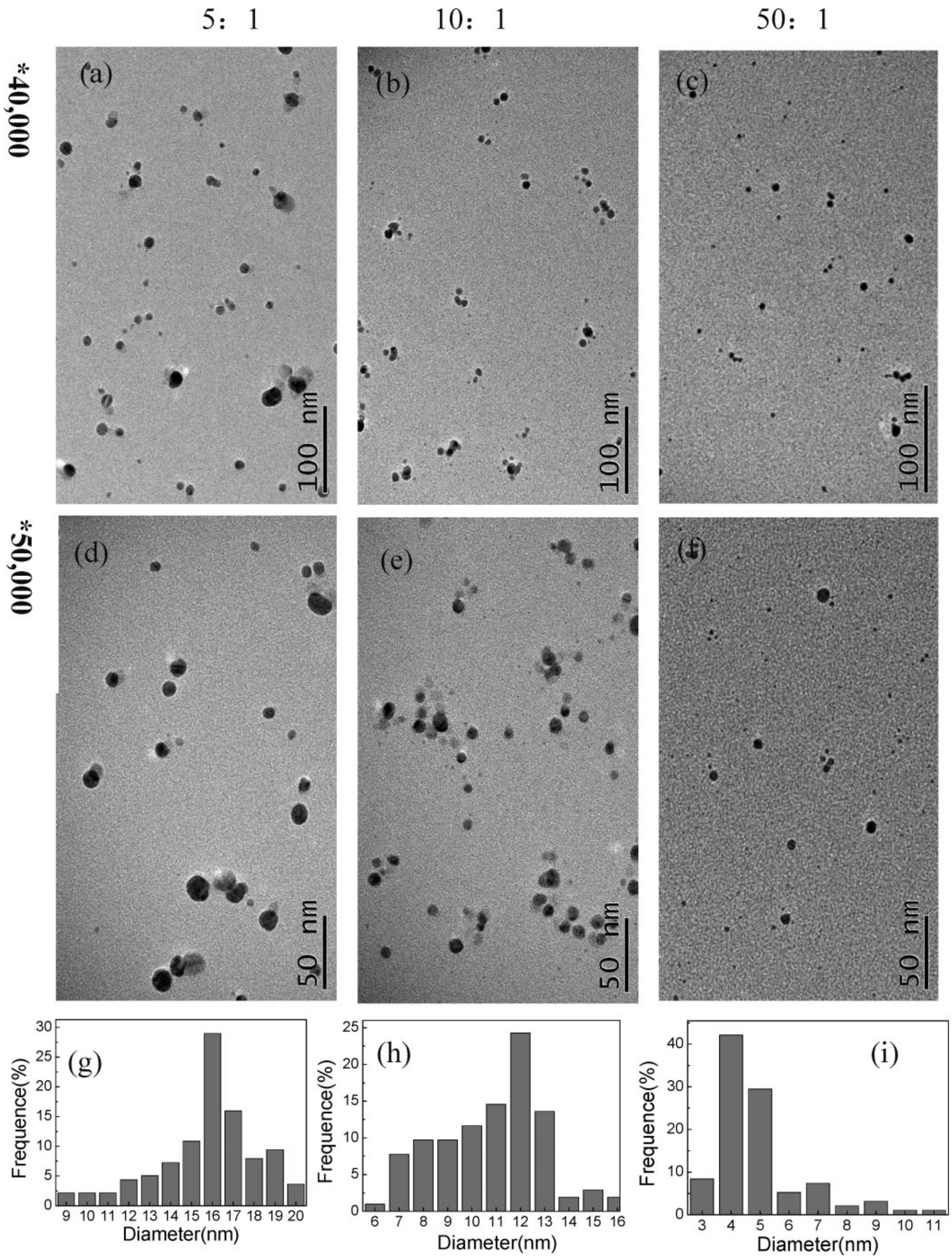

Figure 5. Transmission emission microscopic images of AgNPs when Dextran/Ag^+ ratio is set to (a) 5:1, (b) 10:1, and (c) 50:1 (with magnifications of 40 000); (d) 5:1, (e) 10:1, and (f) 50:1 (with magnifications of 50 000); and histograms of the size distribution of particles when Dextran/Ag^+ ratio is set to (g) 5:1, (h) 10:1, and (i) 50:1.

3.2. UV–Vis Absorption Spectroscopy and TEM Analysis

UV–Vis absorption spectroscopy is proven to be a sensitive method to evaluate silver colloids: silver nanoparticles exhibit an intense absorption peak due to the surface plasmon resonance (SPR) excited by certain wavelengths of incident light.[29] The UV–Vis absorption spectra of AgNP colloids synthesized with different reaction times are shown in Figure 3a. In this condition, dextran monomer/Ag^+ molar ratio of 5:1 were used. The SPR absorption band was observed around 396 nm. With increasing process time, the samples show higher absorbance peaks, indicating the increase of AgNPs concentration and the narrow size distribution of the synthesized nanoparticles. Figure 3b shows the absorbance intensity at 396 nm for Ag NPs increases at a high rate and saturates at approximately 25 min. This is because at the beginning, the silver cations are immediately reduced, resulting in a high growth rate. With increasing reaction time, more free silver cations have been reduced by plasma, and absorbance intensity becomes saturated when all the available cations are consumed.

Dextran is a water-soluble polysaccharide. It is produced industrially in a large scale and has a wide range of applications in food and medical related areas. The utility of dextran and its amino derivative as capping agents and reduction agent have been reported in various preparatory methods for silver nanoparticle generation.[29,30] The influence of dextran concentration on silver nanoparticle size was studied through UV–Vis spectroscopy and TEM. Figure 4 shows the UV–Vis absorption spectra of the AgNPs containing electrolytic solutions with dextran monomer/Ag^+ molar ratios (for simplicity, referred to as Dextran/Ag^+ ratio from here on) of 5:1, 10:1, and 50:1, respectively, obtained at the same reaction time of 5 min. In the case of lower molar ratio (5:1), the SPR band was observed at 396 nm. When the ratio was increased to 10:1 and 50:1, the band becomes more symmetrical, and a blue shift in the peak of the SPR band appears. These features are associated with the small size and uniform size distribution of the silver nanoparticles synthesized.

TEM images were used to investigate the shape and size distribution of the AgNPs. The TEM pictures with different dextran/Ag^+ ratio were taken with magnifications of 40 000 (Figure 5a–c) and 50 000 (Figure 5d–f), respectively. In general, the particles were spherical in shape and well dispersed in the solution. The size distribution histograms (Figure 5g–i) showed that these particles were with average diameters of 16.49 ± 2.98, 11.16 ± 2.23, and 5.34 ± 1.44 nm, corresponding to Dextran/Ag^+ ratios of 5:1, 10:1, and 50:1, respectively (based on 200 NPs). TEM results were consistent with the results from the UV–Vis absorption spectra. The higher Dextran/Ag^+ ratio in theory should produce ultrafine AgNPs. However, the high dextran concentration also makes the electrolyte more viscous and therefore affects plasma discharge. We therefore set the Dextran/Ag^+ ratio to 10:1 for subsequent experiments, in which the AgNPs were collected after a 25-min reaction.

3.3. FTIR Analysis

The FTIR spectra of dextran and dextran-coated silver nanoparticles are shown in Figure 6. The absorption peaks at 3 319 and 1 655 cm^{-1} in the dextran spectrum are due to the OH-stretching and HOH-bending modes of residual water. A C—H stretching mode was evident at 2 926 cm^{-1}

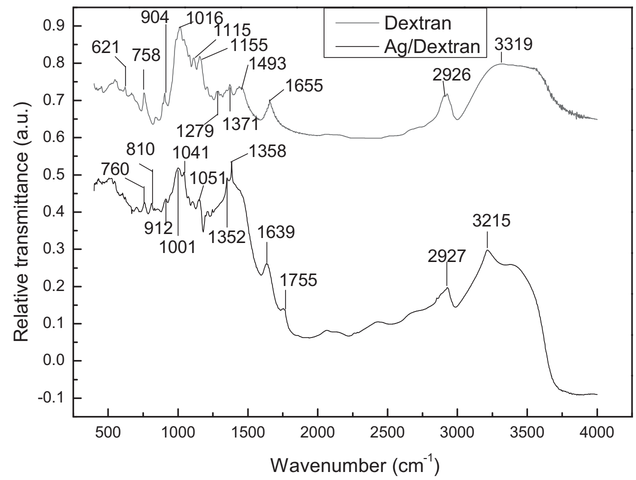

Figure 6. FTIR spectra of pure dextran and dextran coated AgNPs.

plus a cluster of additional features in the "fingerprint" region below 1 500 cm^{-1}, including a strong C—O response at 1 016 cm^{-1}. The FTIR spectrum of the dextran-coated silver nanoparticles also exhibited the dextran signature, but with a slight spectrum shift and a C=O response at 1 755 cm^{-1}. The high-energy electrons in the plasma

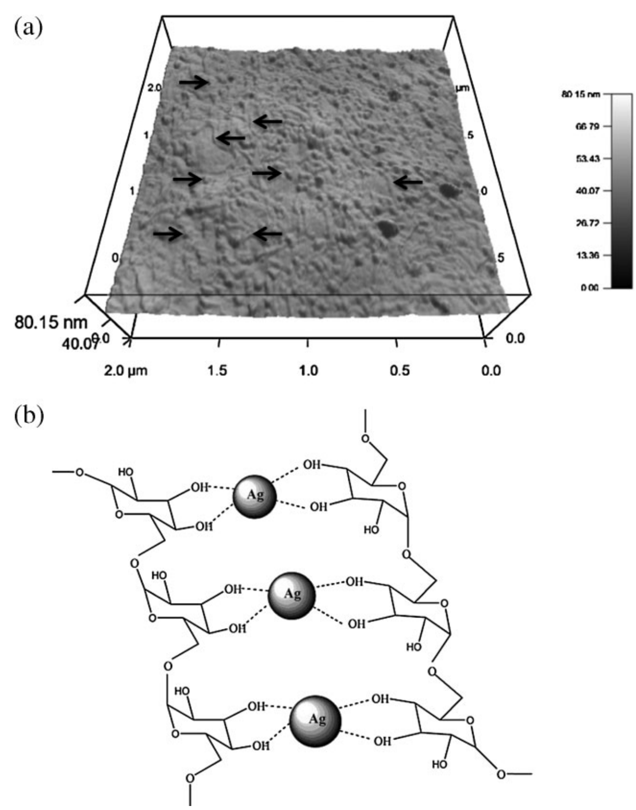

Figure 7. (a) 3D AFM image of AgNPs entrapped by dextran molecules; (b) A schematic diagram showing the coordination bond between the dextran molecules and AgNPs.

DOI: 10.1002/ppap.201300038

initiated the single- or multiple-step ionization and excitation of species in the Ar and liquid.[31] Of all the plasma-activated species induced liquid ionization to generate reactive oxygen species (ROS) such as ozone, atomic oxygen, superoxide, peroxide, and hydroxyl radicals. We deduce that these were contributed to the oxidation of C—O to C═O.

3.4. AFM Analysis

Dextran is used as a protecting agent as well as a reduction agent for the synthesis of metal nanoparticles.[28] The coating of dextran to the nanoparticle surface ensures a high level of biocompatibility, enabling the as-produced particles to be used directly for biological applications without further surface functionalization. The AFM analysis of the synthesized AgNPs is shown in Figure 7a. The 3D AFM image shows the well dispersed spherical silver nanoparticles (left arrows) surrounded by dextran molecules (right arrows). The synthesized AgNPs nanoparticles are coordinated with hydroxyl group of dextran molecules which in turn prevents their large-scale aggregation. The schematic diagram in Figure 7b shows that AgNPs are entrapped by the hydroxyl groups in the dextran molecules.

3.5. Antimicrobial Activity of Ag NPs against Microorganism

Antimicrobial tests are performed against *E. coli* (gram-negative) and *S. aureus* (gram-positive) in liquid by adding different concentrations of AgNPs (1.5, 3.2, 6.4, 12.5, 25, 50, and 100 $\mu g\ ml^{-1}$). The optical density (OD) of the solutions as a function of time was measured periodically up to 16 h, to indicate the bacterial growth. Figure 8a and b shows the growth curves of *E. coli* treated with various concentrations of AgNPs with initial bacteria concentrations of 10^6 and 10^8 CFU ml^{-1}, respectively. Three phases are involved during the bacterial growth: lag phase, exponential phase, and stabilization phase. Without AgNPs, *E. coli* reached exponential phase rapidly for both initial bacteria concentrations. In the 10^6 CFU ml^{-1} group, when exposed to 1.5 and 3.2 $\mu g\ ml^{-1}$ silver nanoparticles, *E. coli* cells began to grow after 12 and 14 h, respectively. In the 10^8 CFU ml^{-1} group, when exposed to 1.5, 3.2, and 6.4 $\mu g\ ml^{-1}$ of AgNPs, *E. coli* cells are lagged to 4, 6, 8 h, respectively. Other higher concentrations show no bacterial growth within 16 h. Figure 8c and d shows the growth curves of *S. aureus* treated with AgNPs with initial concentration of 10^6 and 10^8 CFU ml^{-1}, respectively. *S. aureus* is much more difficult to kill due to the significant difference in cell wall structures as compared to the gram-negative *E. coli*. For the 10^6 CFU ml^{-1} group, inhibition is observed when the AgNP concentration is increased to 6.4 $\mu g\ ml^{-1}$. For the 10^8 CFU ml^{-1} group, *S. aureus* cells are lagged to 9 h when exposed to 12.5 $\mu g\ ml^{-1}$ AgNPs. Further increase of AgNP concentration led to complete inhibition of bacterial growth.

To further support the OD measurement mentioned above, the number of bacteria colonies grown on nutrient agar plates was evaluated as a function of the concentration of AgNPs and shown in Figure 9. With a bacterial concentration of 10^6 CFU ml^{-1}, the minimum inhibitory

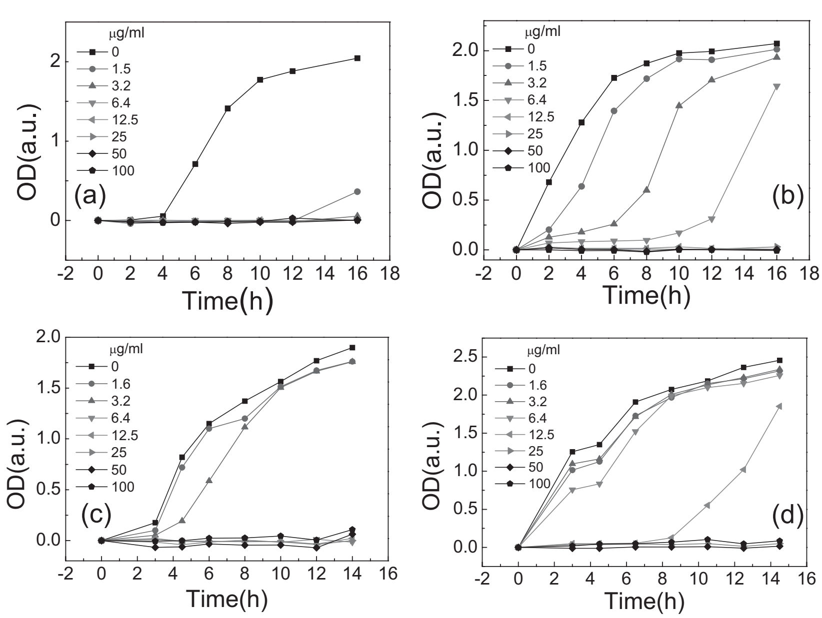

Figure 8. Effect of different concentrations of AgNPs on the growth of *E. coli* at (a) 10^6 CFU ml^{-1} and (b) 10^8 CFU ml^{-1}, respectively, and of *S. aureus* at (c) 10^6 CFU ml^{-1} and (d) 10^8 CFU ml^{-1}, respectively. (OD is measured at 600 nm).

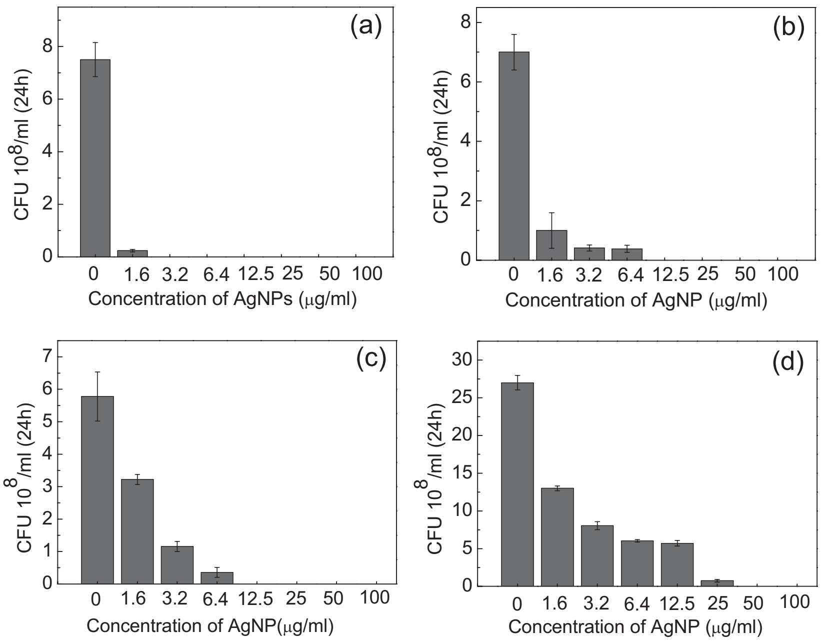

Figure 9. MIC evaluation by CFU counting as a function of AgNP concentration in solution: (a) and (b) are for *E. coli* at initial concentrations of 10^6 and 10^8 CFU ml^{-1}, respectively; (c) and (d) are for *S. aureus* at initial concentration of 10^6 and 10^8 CFU ml^{-1}, respectively.

concentrations for *E. coli* and *S. aureus* are 1.6–3.2 and 6.4–12.5 $\mu g\ ml^{-1}$, respectively. While with a bacterial concentration of 10^8 CFU ml^{-1}, the minimum inhibitory concentrations for *E. coli* and *S. aureus* are 3.2–6.4 and 12.5–25 $\mu g\ ml^{-1}$, respectively. The bacterial growth inhibition trend observed from CFU data is consistent with the OD measurements.

4. Conclusions

Silver nanoparticles decorated with dextran were synthesized by a simple and environmentally benign method using microplasma reduction. A growth mechanism of the AgNPs assisted by microplasma was proposed. The nanoparticles' distribution, sizes and morphology were well characterized and the particles' size is controllable by adjusting the composition of the electrolytic solution. The resulting AgNPs showed strong antibacterial property against *E. coli* and *S. aureus*. It was found that the antibacterial activity of AgNPs was associated with bacterial type and initial bacterial concentration. Their superior antibacterial activity and environmental friendly preparation give them potential applicability in bioengineering and other fields.

Acknowledgements: This work is sponsored by the Bioelectrics Inc. (USA). The authors want to thank Dr. Hao Wang of College of Engineering at Peking University for his help with AFM. Acknowledgement is also made to Xiaosen Li of the Chemical Engineering department at Tsinghua University for his help with FTIR spectroscopy.

Received: April 1, 2013; Revised: July 22, 2013; Accepted: September 16, 2013; DOI: 10.1002/ppap.201300038

Keywords: Bacterial disinfection; Microplasma; Silver nanoparticles

[1] S. Silver, L. T. Phung, *Annu Rev Microbiol.* **1996**, *50*, 1.
[2] H. J. Klasen, *Burns.* **2000**, *26*, 2.
[3] R. M. Slawson, M. I. Van Dyke, H. Lee, J. T. Trevors, *Plasmid* **1992**, *27*, 1.
[4] C. A. D. Santos, A. F. Jozala, P. A. Junior, M. M. Seckler, *J. Nanobiotechnol.* **2012**, *10*, 43.
[6] M. Fondevila, R. Herrer, M. C. Casallas, L. Abecia, J. J. Ducha, *Anim. Feed Sci. Technol.* **2009**, *150*, 3.
[7] I. Perelshtein, G. Applerot, N. Perkas, G. Guibert, S. Mikhailov, A. Gedanken, *Nanotechnology* **2008**, *19*, 245705.
[8] J. Y. Song, E. Y. Kwon, B. S. Kim, *Korean J. Chem. Eng.* **2012**, *29*, 12.
[9] A. Panacek, L. Kvtek, R. Prucek, M. Kolar, R. Vecerova, N. Pizurova, V. K. Sharma, T. Nevecna, R. Zboril, *J. Phys. Chem. B.* **2006**, *110*, 16248.
[10] Y. T. Zhang, Y. Guo, M. A. T. Cai, *Chin. Phys. Lett.* **2011**, *28*, 10.
[11] B. S. Yin, H. Y. Ma, S. Y. Wang, S. H. Chen, *J. Phys. Chem. B.* **2003**, *107*, 34.
[12] M. B. Ahmad, M. Y. Tay, K. Shameli, M. Z. Husssein, J. J. Lim, *Int. J. Mol. Sci.* **2011**, *12*, 8.
[13] A. Sileikaite, J. Puiso, I. Prosycevas, S. Tamulevicius, *Mater. Sci.* **2009**, *15*, 1.
[14] W. S. Seo, T. H. Kim, J. S. Sung, K. C. Song, *Korean Chem. Eng. Res.* **2004**, *42*, 78.
[15] S. Kheybari, N. Samadi, S. V. Hosseine, A. Fazeli, M. R. Fazeli, *Daru* **2010**, *18*, 3.
[16] K. Satyavani, S. Gurudeeban, T. Ramanathan, T. Balasubramanian, *Avicenna J. Med. Biotechnol.* **2012**, *4*, 1.
[17] K. Harada, S. Suzuki, *Nature* **1997**, *266*, 5599.
[18] P. Bruggeman, C. Leys, *J. Phys. D Appl. Phys.* **2009**, *42*, 5.
[19] T. Kaneko, K. Baba, R. Hatakeyama, *J. Appl. Phys.* **2009**, *105*, 10.
[20] K. H. Becker, K. H. Schoenbach, J. G. Eden, *J. Phys. D* **2006**, *39*, 3.
[21] P. Kurunczi, J. Lopez, H. Shah, K. Becker, *Int. J. Mass Spectrom.* **2001**, *205*, 277.
[22] I. G. Koo, M. S. Lee, J. H. Shim, J. H. Ahn, W. M. Lee, *J. Mater. Chem.* **2005**, *15*, 38.
[23] J. Hieda, N. Saito, O. Takai, *J. Vacuum Sci. Technol. A* **2008**, *26*, 4.
[24] C. Richmonds, R. M. Sankaran, *APL* **2008**, *93*, 131501.
[25] S. Sato, K. Mori, O. Ariyada, H. Atsushi, T. Yonezawa, *Surf. Coat. Technol.* **2011**, *206*, 5.

[26] X. Z. Huang, X. X. Zhong, Y. Lu, Y. S. Li, A. E. Rider, S. A. Furman, K. Ostrikov, *Nanotechnology* **2013**, *24*, 095604.
[27] M. Miryajani, A. Ghassempour, A. Aliahmaded, *J. Peptide Sci.* **2011**, *16*, 1.
[28] K. P. Bankura, D. Marity, M. M. R. Mollick, D. Mondal, B. Bhowmick, M. K. Bain, A. Chakraborty, J. Sarkar, K. Acharya, D. Chattopadhyay, *Carbohydr. Polym.* **2012**, *89*, 4.
[29] Y. Ma, N. Li, C. Yang, X. R. Yang, *Anal. Bioanal. Chem.* **2005**, *382*, 1044.
[30] Y. Q. Ma, J. Z. Yi, L. M. Zhang, *J. Macromol. Sci.* **2009**, *46*, 6.
[31] F. X. Liu, P. Sun, N. Bai, Y. Tian, H. X. Zhou, S. C. Wei, Y. H. Zhou, J. Zhang, W. D. Zhu, K. H. Becker, J. Fang, *Plasma Process. Polym.* **2010**, *7*, 3.